Impact of Wind Farm Frequency Control on the Dynamic Response of the All-Island Irish System

Francesca Madia Mele, Federico Milano
School of Electrical & Electronic Engineering
University College Dublin
Belfield, Ireland

David Cashman, Jonathan O'Sullivan
EirGrid
Dublin, Ireland

***Abstract*—This work originates from the observation that the current practice for wind farm frequency control mandated by the Irish Grid Code can lead to significant frequency oscillations in the system. With this regard, the paper proposes a variety of solutions to mitigate such an oscillatory response of wind farms and recover the frequency. The test case focuses on the trip of the largest HVDC interconnector and considers projected dispatch scenarios. The case study is based on a realistic although simplified dynamic model of the all-island Irish system.**

I. Introduction

In the last decade, a number of national system operators have included in their Grid Codes frequency and active power requirements for wind farms, which have to enable voltage and frequency support and control. In Europe, some examples are the Irish [1], the Danish [2], and the German [3] regulations. These documents impose that, along with the requirements for the steady-state behavior, every wind farm has to provide primary frequency regulation.

The most common techniques for primary frequency control provided by wind farms are based on pitch angle control [4]; Rate of Change of Frequency (ROCOF) [5]; and droop control [6], [7]. A review and a comparison of the dynamic performance of these techniques are provided in [8]. In the Irish system, the active power output of wind turbines is defined as the active power set point requested by the grid operator and adjusted through a frequency droop control [1].

The Irish Grid Code also defines a specific power-frequency response curve (see Fig. 1) for wind farm frequency controllers [1]. The curve includes a deadband, which reduces the stress on the turbine controllers by allowing a relatively small fluctuation of the frequency around its nominal value [9]. Outside the deadband, the response of the wind farm follows a 4% droop calculated with respect to the nominal frequency, thus leading to the steps around 50 Hz shown in Fig. 1.

Unfortunately, the deadband, as any non-linearity has the potential to, can lead to an undesired oscillatory behavior. Early in 2016, following a trip of the East-West Interconnector (EWIC) that was exporting power to UK, persistent oscillations of both the system frequency and the power output of a 84 MW, 110 kV wind farm located in Ireland were observed (see Fig. 2).

This paper proposes control-based solutions to mitigate the aforementioned oscillations due to the frequency control of wind farms. The case study also presents an up-to-date evaluation of the dynamic performance of the all-island Irish system.

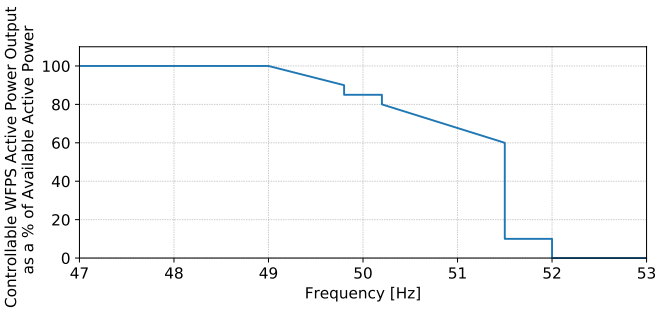

Figure 1: Power-frequency response curve defined in the Irish Grid Code.

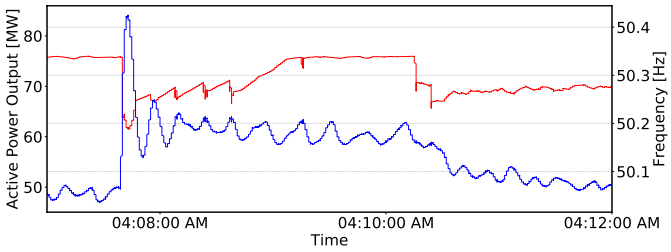

Figure 2: Dynamic response of the Irish system following the loss of the EWIC interconnector. Red line: wind farm active power output; blue line: frequency.

The controllers proposed in this paper are consistent with those in the literature and are compatible with those currently used in Ireland, as follows.

- An adaptive droop that varies according to the frequency deviation [10].
- A properly tuned PI controller, which ensures the convergence of the frequency to its nominal value [11].
- An hysteresis controller that effectively adjusts the active power output of the wind turbine and support frequency recovery [12].

The remainder of the paper is organized as follows. Section II presents the conventional and the proposed primary frequency controllers. Section III discusses the case study based on a simplified dynamic model of the all-island Irish system. Conclusions are drawn in Section IV.

II. Conventional and Proposed Primary Frequency Controllers

This section outlines conventional and proposed primary frequency controllers considered in the case study of the paper. The controllers are:

- Synchronous machine turbine governor with inclusion of a deadband;
- Active power output controller for wind turbines including deadband and standard droop controller;
- Active power output controller for wind turbines including deadband and variable droop controller;
- PI controller; and
- Hysteresis-based controller.

A. Synchronous machine turbine governor with deadband

In a conventional power system, the primary frequency regulation is based on synchronous machine turbine governors. The use of a deadband to avoid excessive regulation, along with the droop settings specified by the system operators, is a common practice adopted in conventional and non-conventional power plants all over the world [1], [13], [14]. In the case study of this paper, values of the synchronous machines droop, which describes the change in frequency with load, range from 2% to 4% [15].

B. Constant droop controller

Whilst in conventional power plants the inertial response and the governor control attain the frequency regulation, in wind farms such regulation is achieved by varying the injection of active power into the system [6], [7].

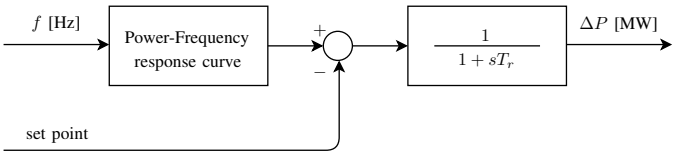

Figure 3: Wind farm droop controller.

The block diagram in Fig. 3 shows the droop controller of the wind farm considered in the simulations. This varies the active power output of the wind farm according to the instantaneous value of the frequency. Based on the power-frequency curve shown in Fig. 1, if the frequency lies within the deadband limits, the controller provides a specified margin by generating less power than what is available from the wind. In this system setup, the actual power generated, namely *set point* in Fig. 3, is the 85% of the available power. If the frequency goes beyond the deadband limits, i.e., $49.8 - 50.2$ Hz (± 200 mHz), the control calculates the power order as a function of the governor droop controller, which is determined by means of the power-frequency response curve.

In this study, the droop (i.e., the slope of the response curve outside the deadband range) is calculated from the center-point of the deadband, resulting in a step response when the limits are exceeded. Formally, the droop is defined as [16]:

$$\text{droop}_{\%} = \frac{\Delta f}{f_N} \cdot \frac{P_N}{\Delta P} \cdot 100 \tag{1}$$

where Δf is the frequency deviation, and f_N is the nominal frequency of the system, ΔP is the change in active power of the wind farm, and P_N is the capacity of the wind farm. The droop default value is 4% when operating outside the deadband range. The set point and the governor droop are calculated with respect to the registered capacity of the system.

The output provided by the controller is ΔP in MW. This is obtained as the difference between the power output calculated with respect to the actual frequency of the system and the active power set point, then processing this difference through a simple lag with a time constant T_r. The simple lag determines the ramp rate limit imposed on changes to power order signal. In this setup, $T_r = 0.15$ s.

C. Variable droop controller

As discussed in the previous section, the droop of wind farm controllers is typically a constant coefficient set by the TSO. However, reference [10] shows that a variable droop that adapts to system operating conditions can improve the dynamic response of the wind farm and the overall system. Such a variable droop is calculated directly proportionally to the ROCOF, i.e., the rate of change of frequency of the system. Hence, the slope of the power-frequency characteristics changes depending on both the frequency variation and the magnitude of the contingency occurring.

D. PI controller

The PI controller considered in this work processes the ΔP obtained as the output of the simple lag shown in Fig. 3. The main added value of the PI controller is that it provides a perfect tracking of the input signal [11]. In this case, the deadband is thus necessary to prevent wind farms to take over the frequency regulation of the whole system. A properly tuning of the PI parameters is also crucial to obtain an acceptable dynamic response. This is thoroughly discussed in the case study.

E. Hysteresis controller

A wind farm power control based on a hysteresis controller has been recently proposed in [12]. The scheme of the hysteresis control considered in this paper is shown in Fig. 4. Such a control evaluates the instantaneous value of the frequency, and provides a specified active power margin according to the droop function if this value increases above the *Switch on* threshold. The control remains active until the frequency drops below the *Switch off* threshold.

The controller works on the input signal of the Power-Frequency characteristics of Fig. 1, it provides a more aggressive regulation with respect to constant droop controller. In the case study, *Switch on* = 50.2 Hz and *Switch off* = 50.015 Hz are used.

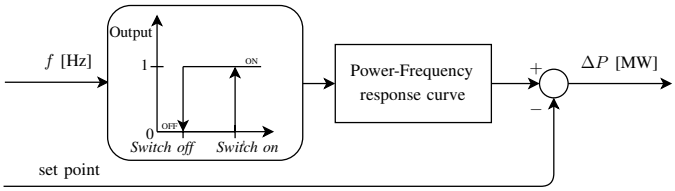

Figure 4: Droop controller with inclusion of a hysteresis block.

III. Case Study

The performance of the controllers described in Section II is compared in this section. The test-bed consists of a simplified dynamic model including conventional synchronous generators, i.e., Combined Cycle Gas Turbines (CCGT), Open Cycle Gas Turbines (OCGT), and pumped storage; wind turbines; HVDC interconnectors; and static reserve sources and loads [17]. To have a representation closely resembling the Ireland and Northern Ireland System, the following devices have been modeled:

- 53 unit models, based on different technologies, including steam turbines, OCGT, CCGT, hydroelectric;
- A pumped storage model including a hydro governor model representing pumping, ramp constraints and trip control;
- 2 HVDC interconnectors (i.e., EWIC, Moyle) totaling $1,000$ MW;
- Contracted interruptible loads;
- Load variation response with frequency and total dispatch; and
- A wind generation model enabled with ROCOF protections, governor control, droop control, inertial response, and fault ride through.

The model setup considers both historical dispatches comprising export through the EWIC, as well as projected 2018 and 2020 cases, based on [15] and [18]. Simulated scenarios include wind energy export up to 500 MW, different levels of non-synchronous penetration ranging from 10% to 75%, as well as wind power generated ranging from 500 MW to $4,000$ MW. Forecast dispatch cases are taken from Plexos models, the following are the constraints considered: for the 2018 scenario, 65% of the total power production is provided by wind, ROCOF constraint of 1 Hz/s over 500 ms, inertia constraint of $17,500$ MW, and minimum 7 units online; for the 2020 scenario, no reserve constraints, no ramp constraints, 75% of the total power production is provided by wind, ROCOF constraint of 1 Hz/s over 500 ms, and minimum 5 units online. In the results, every active power is normalized with respect to the total installed capacity, i.e., $10,000$ MW, as expected by 2020 [19].

The contingency analyzed is the trip of the HVDC interconnector in exporting mode, occurring at $t = 1$ s. In the Irish system, in fact, the loss of a large load in the form of an exporting interconnector can be a more significant contingency than the loss of a large generation unit.

A. Base Case

Figure 5 shows the trajectories for the base-case scenario, which includes no wind farm frequency control. Those reaching the highest zenith are related to the dispatches characterized by the bigger ΔP and the lower conventional generation provided by the system. Although the frequency settles after $10-15$ s depending on the overshoot experienced, the zenith is, in most of the cases, unacceptable. Therefore, the adoption of a controller able to mitigate Δf and to recover the frequency within acceptable limits is essential.

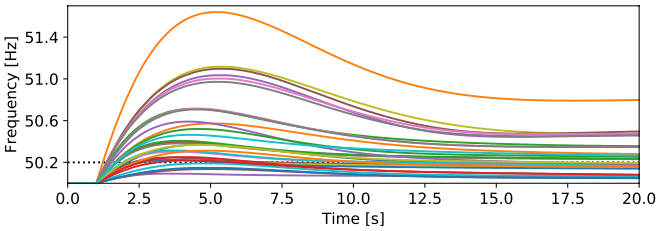

Figure 5: Frequency of the system without wind farm frequency control, 30 dispatches.

B. Constant droop controller

With the inclusion of the droop control and deadband, the frequency behavior shows an improvement in terms of frequency zenith. The vast majority of the trajectories reaches the zenith within 1 s after the contingency. During the transient, however, the frequency oscillates around the deadband limit and finally settles after $2-4$ s (see Fig. 6).

The cyclic behavior of the wind farm power output is due to the step at the edge of the deadband characteristic (see Fig. 1), the trend is triggered by the frequency crossing the limit of the deadband. Therefore, the width of the deadband is crucial: the smaller the deadband, the smaller the jump on its edge, the smaller the magnitude of the oscillations of the response.

Figure 7 shows two different settings applied to a scenario with 68% of non-synchronous generation, $4,141$ MW generated by wind, 495 MW imported, and 6 units online.

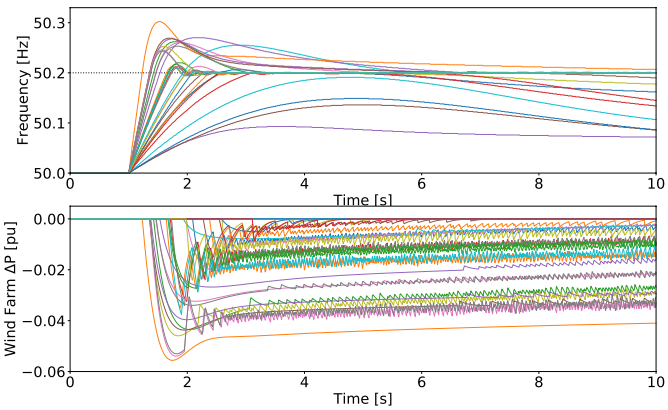

Figure 6: Constant droop controller, 30 dispatches.

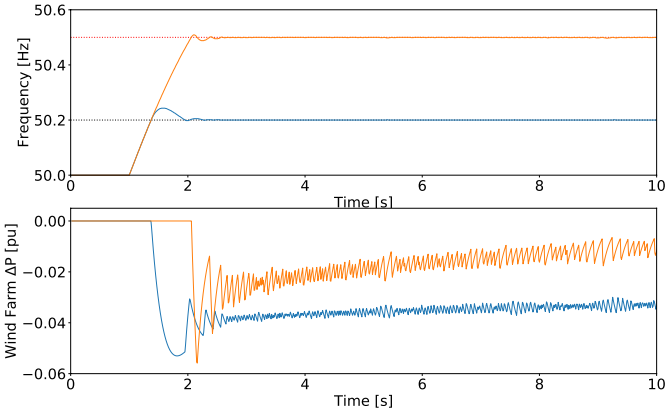

Figure 7: Constant droop controller with different deadband widths. Blue line: 200 mHz deadband, orange line: 500 mHz deadband.

The system frequency and the wind farm power output are depicted for values of the deadband of 200 mHz (blue line) and 500 mHz (orange line). The latter is an arbitrary choice. As expected, a wider deadband results in larger oscillations in the wind farm response. This oscillatory behavior is undesirable in a power system as it could cause instability in other units experiencing the frequency changes. The wind farm oscillations could be magnified by other units which can result in overall system stability issues. Similarly, this type of chattering would be undesirable for a wind turbine as it could result in increased wear and tear.

C. Variable droop controller

The overall outcome related to this controller is similar to the previous case. Figure 8 shows the advantage of the variable droop controller: all trajectories settle on the deadband in about 1 s, and all of them are recovered within the deadband. On the other hand, a persistent oscillation of the frequency occurs around the deadband limit before recovering inside the band.

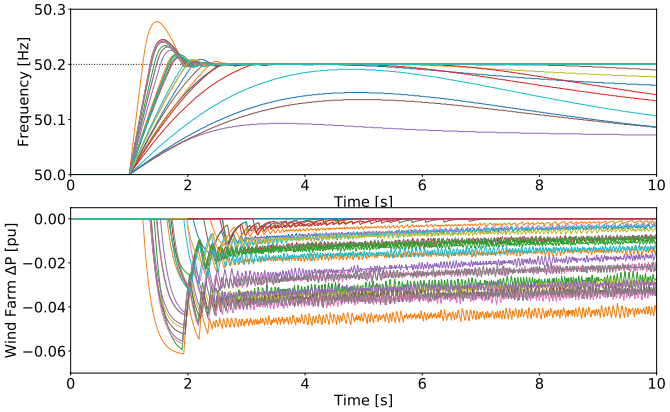

Figure 8: Variable droop controller, 30 dispatches.

D. PI Controller

Based on several simulations ranging the PI parameters from 0 to 2, the variation of K_p and K_i from 0.5 to 1 affects the system dynamic in terms of overshoot and the oscillatory behavior of the frequency. Figures 9 and 10 show the effects of the variation of K_p and K_i respectively. Simulation refers to the scenario consisting of 69% of non-synchronous generation, $2,928$ MW generated by wind, 606 MW imported, 7 units online.

For $K_p = 0.5$, the zenith is about 50.3 Hz and the frequency recovers inside the deadband and very close to the nominal frequency (i.e., about 50.05 Hz) in about 5 s. Increasing K_p to 1, the zenith is reduced to 50.25 Hz, and the frequency recovers after oscillating around the deadband upper limit for about 4 s. Hence, the bigger K_p, the smaller the overshoot, and the higher the steady-state error after the contingency.

Ranging K_i from 0.5 to 1, the overshoot of the frequency is not impacted and the zenith is 50.25 Hz. However, the persistent oscillatory behavior of the frequency around the upper deadband limit is improved. The bigger K_i, the faster the response of the system in recovering the frequency, and the less the oscillations of both frequencies and wind farm

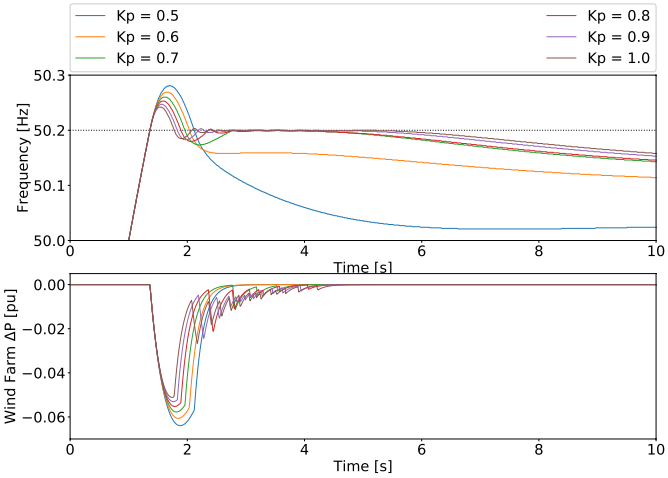

Figure 9: PI controller, sensitivity analysis with respect to K_p gain.

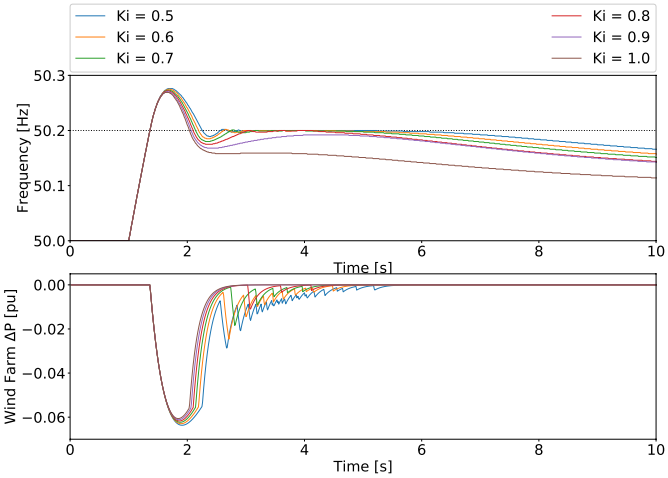

Figure 10: PI controller, sensitivity analysis with respect to K_i gain.

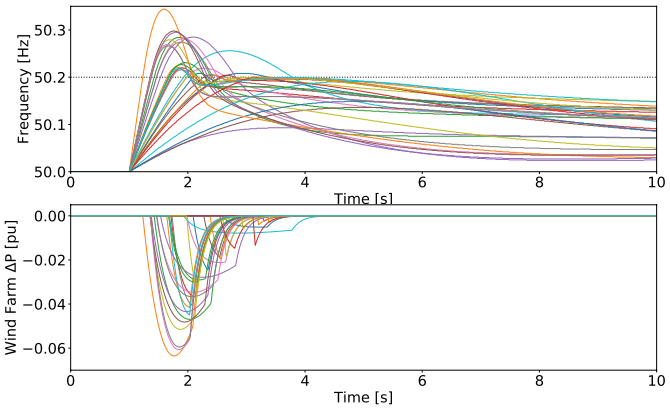

Figure 11: PI controller, 30 dispatches. $K_p = 0.6$ and $K_i = 1$.

power output.

Figure 11 shows the simulations of the 30 dispatch cases for $K_p = 0.6$ and $K_i = 1$. These recommended values reduce the oscillations of the wind farm power output, mitigate the excessive overshoot of the frequency and recover it relatively close to its nominal value (i.e., 50.1 Hz) in 2.5 s.

E. Hysteresis controller

Figure 12 shows that the inclusion of the hysteresis in the wind farm frequency control entails a considerable reduction of the overshoot for most of the trajectories. Furthermore, the oscillatory behavior shown in the previous cases completely disappears due to the operating principle of this controller. On the other hand, not all the trajectories are recovered within the deadband, and the steady-state error is relatively bigger with respect to the results obtained with the other controllers proposed. Frequencies reach the steady-state in $2-3$ s, so this strategy is a bit slower comparing with the previous presented.

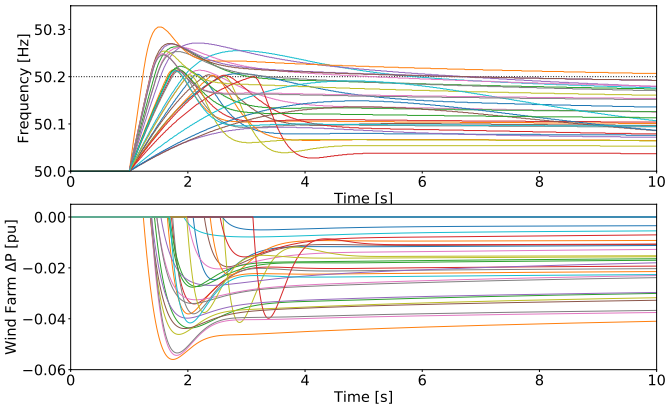

Figure 12: Hysteresis controller, 30 dispatches.

IV. Conclusions

This paper illustrates that the wind farm frequency control can improve the response of the all-island Irish system. This control reduces the zenith of the frequency following a contingency. However, an undesired oscillation due to the deadband of the power-frequency curve mandated in the Irish Grid Code may also occur.

To reduce the impact of the deadband, three different primary frequency controllers are analyzed in the paper. Each controller is able to damp oscillations and recover the system frequency within the deadband limits in less than 5 s. From the grid operator point of view, the PI controller is the best. This controller, in fact, is simple and cheap, significantly improves the frequency response, and, if properly tuned, prevents oscillatory behaviors.

Future work will focus on further improve the dynamic response of the all-island Irish system. Other devices capable of providing frequency control, e.g., energy storage systems, will be considered.

References

[1] EirGrid, *EirGrid Grid Code version 6.0*, 2015, [Online]. Available: https://goo.gl/tGnkBW.

[2] Energinet.dk, *Regulations for Grid Connection*, 2016, [Online]. Available: https://goo.gl/VYVwDc.

[3] Tennet TSO GmbH, *Grid Code*, 2015, [Online]. Available: https://goo.gl/z5Lepo.

[4] R. G. de Almeida and J. A. Pecas Lopes, "Participation of doubly fed induction wind generators in system frequency regulation," *IEEE Transactions on Power Systems*, vol. 22, no. 3, pp. 944–950, Aug. 2007.

[5] J. Morren, S. de Haan, W. Kling, and J. Ferreira, "Wind turbines emulating inertia and supporting primary frequency control," *IEEE Transaction on Power Systems*, vol. 21, no. 1, pp. 433–434, Feb. 2006.

[6] E. Muljadi, V. Gevorgian, M. Singh, and S. Santoso, "Understanding inertia and frequency response of wind power plants," in *Proceedings of the IEEE Symposium on Power Electronics and Machines in Wind Applications (PEMWA)*, Denver, CO, July 2012, pp. 1–8.

[7] F. Teng and G. Strbac, "Assessment of the role and value of frequency response support from wind plants," *IEEE Transactions on Sustainable Energy*, vol. 7, no. 2, pp. 586–595, Apr. 2016.

[8] J. Cerqueira, F. Bruzzone, C. Castro, S. Massucco, and F. Milano, "Comparison of the dynamic response of wind turbine primary frequency controllers," in *Proceedings of the IEEE PES General Meeting*, Chicago, IL, July 2017, pp. 1–5.

[9] G. Kou, P. Markham, S. Hadley, T. King, and Y. Liu, "Impact of governor deadband on frequency response of the U.S. Eastern Interconnection," *IEEE Transaction on Smart Grid*, vol. 7, pp. 1368–1377, May 2016.

[10] A. Buckspan, J. Aho, P. Fleming, Y. Jeong, and L. Pao, "Combining droop curve concepts with control systems for wind turbine active power control," in *Proceedings of the IEEE Power Electronics and Machines in Wind Applications (PEMWA)*, Denver, CO, July 2012, pp. 1–8.

[11] M. Andreasson, D. V. Dimarogonas, H. Sandberg, and K. H. Johansson, "Distributed PI-control with applications to power systems frequency control," in *Proceedings of the American Control Conference (ACC)*, Portland, OR, 2014, pp. 3183–3188.

[12] Y. Liu, L. Jiang, Q. H. Wu, and X. Zhou, "Frequency control of DFIG-based wind power penetrated power systems using switching angle controller and AGC," *IEEE Transaction on Power System*, vol. 32, no. 2, pp. 1553–1567, Mar. 2017.

[13] National Grid, *Grid Code - Issue 5, Revision 20*, 2017, [Online]. Available: https://goo.gl/wBn6jr.

[14] NERC, *Reliability Standards for the Bulk Electric Systems of North America*, 2017, [Online]. Available: https://goo.gl/6CnYUY.

[15] EirGrid and SONI, *All-island Generation Capacity Statement 2012-2021*, 2011.

[16] SONI, *WFPS Settings Schedule. Version 6.0*, 2015.

[17] L. Ruttledge, N. W. Miller, J. O'Sullivan, and D. Flynn, "Frequency response of power systems with variable speed wind turbines," *IEEE Transactions on Sustainable Energy*, vol. 3, no. 4, pp. 683–691, Oct. 2012.

[18] EirGrid and SONI, *All-island Generation Capacity Statement 2011-2020*, 2011.

[19] ——, *All-island Generation Capacity Statement 2015-2024*, 2015, [Online]. Available: https://goo.gl/Cj2BYJ.